Research article

polymers advanced technologies

Received: 15 September 2016, Revised: 3 December 2016, Accepted: 5 December 2016, Published online in Wiley Online Library

(wileyonlinelibrary.com) DOI: 10.1002/pat.3993

Improving the water resistance of epoxy–anhydride matrices by the incorporation of bentonite

Guillermina Capiel[a]*, Julieta Uicich[a], Vera Alvarez[b] and Pablo Montemartini[a,c]

Epoxy–anhydride-based polymers are commonly used as a matrix in pipeline systems exposed to water during their in-service life. Water absorption at moderate temperatures and/or at long exposure times could lead to irreversible hydrolysis reaction decreasing considerably the polymer overall performance. A strategy to enhance the barrier properties of epoxy resins is to add nanofillers to traditional matrices. In this work, we added bentonite and chemically modified bentonite to this purpose. Water absorption of the resulting materials at three different temperatures (22°C, 80°C, and 93°C) was studied, and simultaneously, the evolution during the immersion tests of glass transition temperature and flexural modulus was recorded. Long-term gravimetric results showed that composites with chemically modified bentonite produce a delay on the hydrolysis of epoxy–anhydride matrix, which is a relevant result, because of the tough application and uses of the system, from the technological point of view. Copyright © 2016 John Wiley & Sons, Ltd.

Keywords: epoxy–anhydride matrices; clay nanocomposites; water absorption process; hydrolysis

INTRODUCTION

Epoxy-based thermosetting polymers are widely used in industrial applications, where an excellent performance and high resistance to environmental conditions (as UV, moisture, high temperatures, etc.) are required. Humidity or direct water contact are unavoidable in many cases, and considering that epoxy materials are very susceptible to water, a great effort has been performed in both the study of water/moisture effects on thermal and mechanical properties and on the design and optimization of new materials. With this propose, a promising alternative is based in adding fillers to traditional polymer matrices to develop composite materials with enhanced mechanical, thermal, and barrier properties. Clay mineral results are very attractive because of its high aspect ratio, high intercalation chemistry that allows increasing clay-polymer compatibility and low cost.[1–6]

Epoxy–anhydride-based polymers are commonly used in pipeline systems, and one of the most important challenges is to gain a complete understanding of water effects on these materials. Water absorption at moderate temperatures and/or at long exposure times could lead to irreversible hydrolysis reactions.[7,8] Such chemical degradation involves a chain scission process and in consequence, materials suffer a sharp decrease in their cross-linked density resulting in a loss of thermomechanical properties. Degradation effects can cause a total failure in on-service components. Even though this phenomenon has been widely studied, there has not been yet a methodology that allows estimating water aging kinetics.

Many authors[9–11] have reported that nanoclays enhanced mechanical and barrier properties decreasing water diffusion. However, there are some different and almost contradictory results in bibliography. Authors have demonstrated that water diffusivity and maximum or equilibrium water content decrease with increase in clay content. Other authors[12,13] demonstrated that water diffusivity decreases with clay content, but maximum water content shows an increase. On the other hand, several works[14,15] have shown that water diffusivity increase with clay content. However, the effect of clays in polymers that suffer more complex processes under water absorption has not been reported yet. A key point is the dispersion of the clay particles in the matrix. In order to achieve better properties, it is necessary to obtain a totally exfoliated structure; this means that the silicate layers are completely and uniformly dispersed in a continuous polymeric matrix,[16] but the tendency of the particles to agglomerate has been difficult to overcome or has led to thermodynamic unstable mixtures. Therefore, the interlayer structure of intercalated clays is the crucial factor affecting the exfoliation energy necessary for the splitting of the silicate structure to the individual silicate layers.[17]

* *Correspondence to: Guillermina Capiel, Composite Materials Group, Research Institute of Material Science and Technology, INTEMA-CONICET, National University of Mar del Plata, Mar del Plata, Argentina.*
E-mail: guillermina.capiel@fi.mdp.edu.ar

a *G. Capiel, J. Uicich, P. Montemartini*
Structural Composites Group, Research Institute of Material Science and Technology, INTEMA-CONICET, National University of Mar del Plata, Mar del Plata, Argentina

b *V. Alvarez*
Composite Materials Group, Research Institute of Material Science and Technology, INTEMA-CONICET, National University of Mar del Plata, Mar del Plata, Argentina

c *P. Montemartini*
Chemical Engineering Department, National University of Mar del Plata, Mar del Plata, Argentina

The aim of this work was to analyze the effect of clay incorporation on the water exposure process of epoxy–anhydride matrices. The clay content (0, 1, and 3wt%) and the clay type (natural and organo-modified) were also studied. The main idea is that the incorporation of bentonite can produce a reduction on the main damage process of this kind of matrices exposed at high temperatures (higher than 80°C), which is the hydrolysis.

EXPERIMENTAL PROCEDURE

Materials

Epoxy matrix was prepared using an epoxy resin based in diglycidyl ether of bisphenol A (DGEBA; DER 383, Dow Chemical Co.) and a methyltetrahydrophthalic anhydride (MTHPA; LINDRIDE 36 K, LindauChamicals, Inc.) as a hardener. Commercially available bentonite(provided by Minarmco S.A., Argentina) and a chemically modified bentonite with tributyl hexadecyl phosphonium bromide (TBHP)[18] were used as a reinforcement.

Sample preparation

The epoxy–anhydride system (B0) was obtained using stoichiometric quantities of epoxy resin and the curing agent with a mass ratio of 100:88 (epoxy : anhydride). The reactive mixture was homogenized by hand, and then it was poured vertically into a 1-mm thick aluminum mold. The curing cycle included 30 min—105°C isothermal stage, a heating ramp at 5°C/min until 150°C and 30 min—150°C post-curing step.

Modification of bentonite with tributyl hexadecyl phosphonium bromide:2.5 gr of clay were dispersed in 100 ml of deionized water. Then, the aqueous solution of TBHP (3.CEC) of the corresponding concentration was added. The mixture was stirred for 4 hr at 70°C. After that, the suspension was filtered through a Buchner funnel and washed with deionized water until it was free of bromide. The organoclays were dried with a freeze-dry system. The characteristics of clays are presented in Table 1.

The epoxy–anhydride clay composites were prepared by manual mixing of epoxy and the appropriate mass of clay. The mixture was then placed in an ultrasound bath for 10 min at 40°C. After that, the hardener was added. The final mixture was poured into the mold and cured in an oven using the curing cycle described earlier. Two different clays were used: bentonite as received and a chemical modification made with TBHP. Details about bentonite chemical modification can be found in previous work.[19]

The resulting materials will be denoted as B1 (epoxy–anhydride containing 1 wt% in bentonite), B3 (epoxy–anhydride containing 3 wt% in bentonite), BM1 (epoxy–anhydride containing 1 wt% in modified bentonite), and BM3 (epoxy–anhydride containing 3 wt% in modified bentonite). Afterwards, samples of 55 × 12 × 1 mm were cut from the materials obtained.

Nanocomposites morphology

X-ray diffraction (XRD) patterns of neat and modified bentonite and epoxy–anhydride clay composites were obtained from a PAN analytical X'Pert PRO diffractometer (Holland) equipped with a monochromatic CuKα radiation source (λ = 1.5406 Å) operating at 40 kV, 30 mA, at a scanning rate of 1 per min and a step size of 0.02.

The morphology of epoxy–anhydride clay composites was also studied under a transmission electron microscope (TEM) Jeol 100 CX II. Samples of about 100 nm were cut from the rectangular specimens using an ultramicrotome at room temperature.

The materials surface was analyzed by scanning electron microscopy (SEM model JEOL JSM 6460 LV). The samples were previously coated with a thin layer of Au/Pd.

Water uptake

In order to register the mass increase during water immersion, 55 × 12 × 1 mm^3 nominal samples were used. Water uptake was

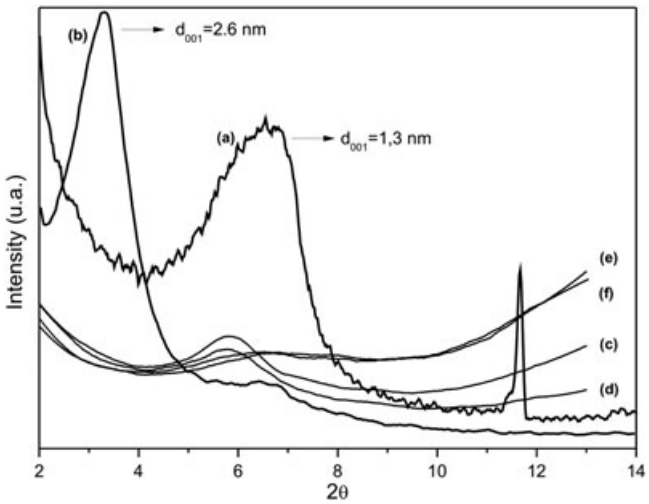

Figure 1. X-ray spectra for (a) bentonite powder, (b) TBHP-modified bentonite powder, (c) epoxy clay composite containing 1 wt% in bentonite (B1), (d) epoxy clay composite containing 3 wt% in bentonite (B3), (e) epoxy clay composite containing 1 wt% in TBHP-modified bentonite (BM1), and (f) epoxy clay composite containing 3 wt% in TBHP-modified bentonite (BM3). TBPH, tributyl hexadecyl phosphonium bromide.

Table 1. Characteristics of used clays

Clay	Organic modifier	Abs. water 24 hr at 90% RH (%)	d_{001} (nm)	Weight loss on ignition (%)	Tp TGA (°C)
Bentonite	None	20.10	1.3	3	—
Bentonite-TBHP	$CH_3(CH_2)_3$–P$^+$(–$(CH_2)_3CH_3$)(–$(CH_2)_3CH_3$)–$(CH_2)_{15}CH_3$	2.73	2.6	29	388.7

TBPH, tributyl hexadecyl phosphonium bromide; RH, Relative humidity; TGA, Temperature of the first peak measured by thermogravimetry.

studied at three different temperatures: 22°C, 80°C, and 93°C. Each curve shows at least five specimens average absorption. In order to obtain the gravimetric data, samples were periodically withdrawn from the water, lived at 21 ± 1°C for 5 min, wiped dry with a tissue paper to remove the surface moisture, and returned into water. The accuracy of the analytical balance used is 10^{-4} g.

The mass change during the absorption tests was dtermined using the following expression:

$$Mass\ \ change\ \ (\%) = \frac{m_t - m_i}{m_i} x100 \qquad (1)$$

where m_t is the sample mass at time t and m_i is the initial sample mass.

Differential scanning calorimetry

Differential scanning calorimetry measurements were performed using a DSC Q2000 from TA Instruments under nitrogen atmosphere in dynamical mode at a constant heating rate of 10°C/min. The experiments were carried out in the temperature range of 30°C to 220°C.

Mechanical properties

Three-point bending tests were performed in an Instron 4467 (Instron, Massachusetts, USA) dynamometer. At least five rectangular specimens ($55 \times 12 \times 1$ mm^3) were tested for each sample. Tests were carried out at room temperature according to American Society for Testing and Materials (ASTM) D790-10 standard.

RESULTS AND DISCUSSION

Nanocomposites morphology

X-ray diffraction and transmission electron microscope

It is known that[20] three main types of composites may be obtained from the interaction between layered silicates and polymer chains: intercalated nanocomposites, exfoliated

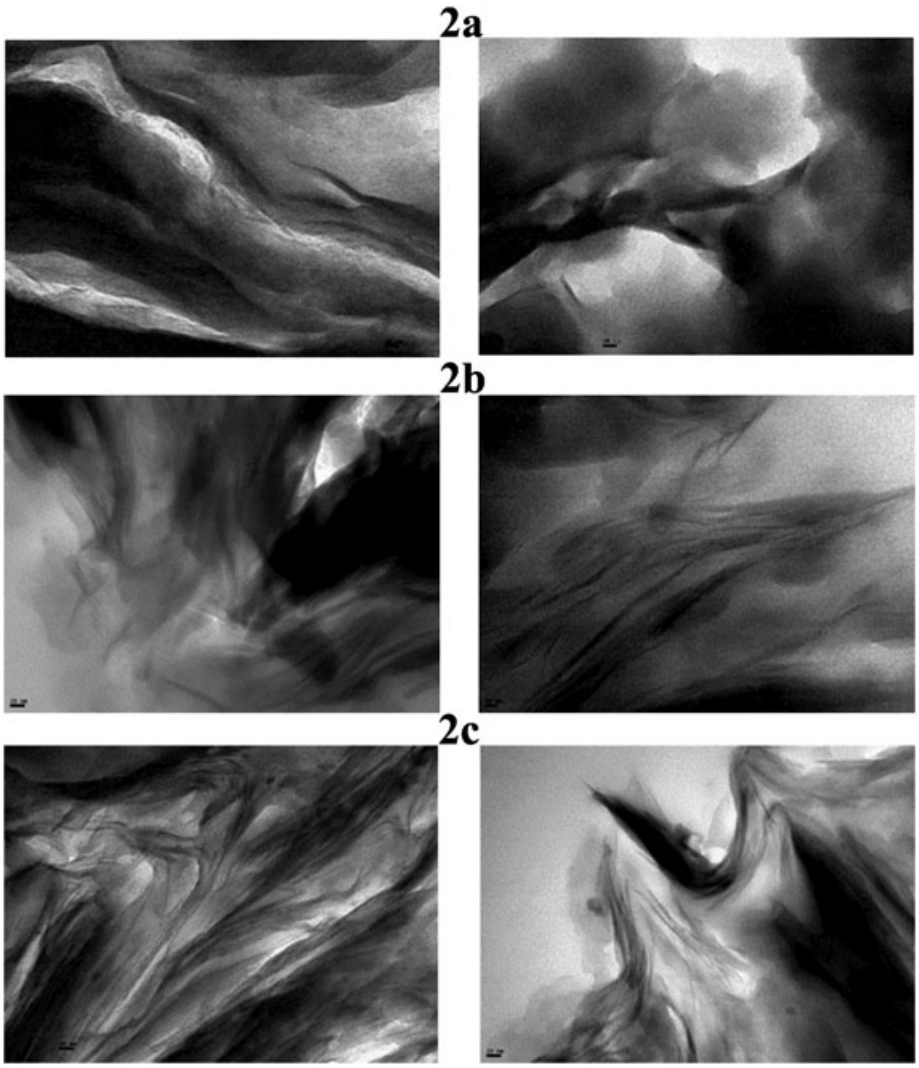

Figure 2. Transmission electron microscope micrographs for composites (a) B1 (left) and B3 (right), (b) BM1, and (c) BM3. Scale bar indicates 20 nm. B1, epoxy clay composite containing 1 wt% in bentonite; B3, epoxy clay composite containing 3 wt% in bentonite; BM1, epoxy clay composite containing 1 wt% in TBHP-modified bentonite; BM3, epoxy clay composite containing 3 wt% in TBHP-modified bentonite; TBPH, tributyl hexadecyl phosphonium bromide.

nanocomposites, and microcomposites. Intercalated structures show regularly alternating layered silicates and polymer chains in contrast to exfoliated structures in which the individual clay layers are delaminated and dispersed in the polymer matrix. These two situations can, however, coexist in the same material. When the polymer is unable to intercalate between the silicate sheets, a traditional microcomposite is obtained.

The critical parameter to achieve the best performance of polymer/clay composites, if clay does not produce defects, is the degree of dispersion of the clay platelets inside the polymeric matrix clay dispersion. X-ray diffractometry was used in order to identify intercalated structures. In such nanocomposites, the repetitive multilayer structure is well preserved, allowing the interlayer spacing to be determined. The intercalation of the polymer chains usually increase the interlayer spacing,

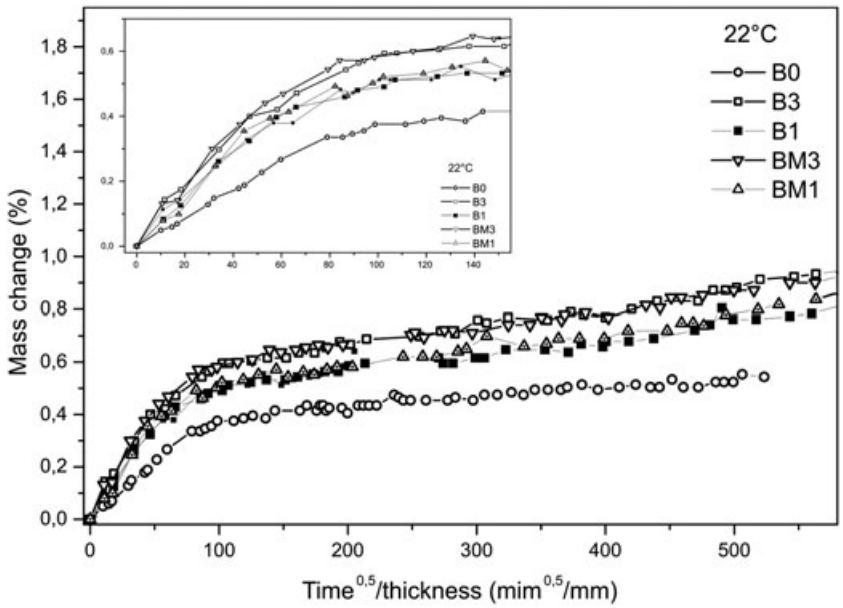

Figure 3. Mass change (%) against reduced exposure time (time$^{0.5}$/thickness) for samples B0, B1, B3, BM1, and BM3 immersed in water at 22°C. B0, neat epoxy–anhydride; B1, epoxy clay composite containing 1 wt% in bentonite; B3, epoxy clay composite containing 3 wt% in bentonite; BM1, epoxy clay composite containing 1 wt% in TBHP-modified bentonite; BM3, epoxy clay composite containing 3 wt% in TBHP-modified bentonite; TBPH, tributyl hexadecyl phosphonium bromide.

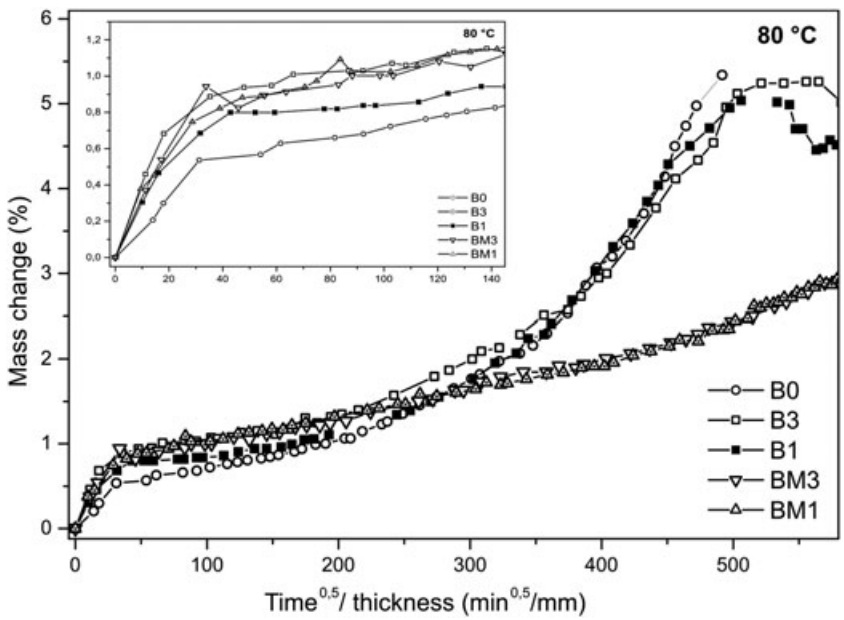

Figure 4. Mass change (%) against reduced exposure time (time$^{0.5}$/thickness) for samples B0, B1, B3, BM1, and BM3 immersed in water at 80°C. B0, neat epoxy–anhydride; B1, epoxy clay composite containing 1 wt% in bentonite; B3, epoxy clay composite containing 3 wt% in bentonite; BM1, epoxy clay composite containing 1 wt% in TBHP-modified bentonite; BM3, epoxy clay composite containing 3 wt% in TBHP-modified bentonite; TBPH, tributyl hexadecyl phosphonium bromide.

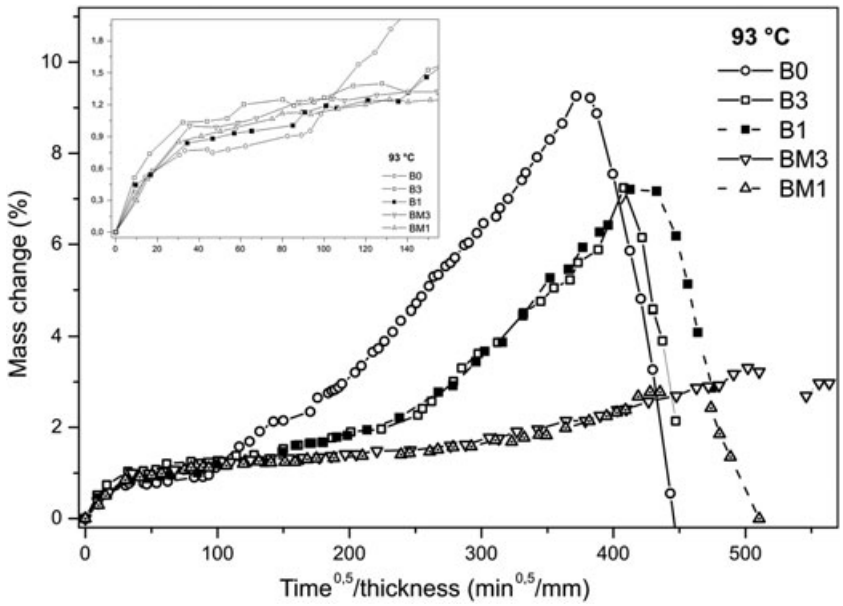

Figure 5. Mass change (%) against reduced exposure time (time$^{0.5}$/thickness) for samples B0, B1, B3, BM1, and BM3 immersed in water at 93°C. B0, neat epoxy–anhydride; B1, epoxy clay composite containing 1 wt% in bentonite; B3, epoxy clay composite containing 3 wt% in bentonite; BM1, epoxy clay composite containing 1 wt% in TBHP-modified bentonite; BM3, epoxy clay composite containing 3 wt% in TBHP-modified bentonite; TBPH, tributyl hexadecyl phosphonium bromide.

leading to a shift in the diffraction peak towards lower angle values. As far as dispersion of clay becomes higher, no more diffraction peaks are visible in the X-ray diffractograms either because of too much large spacing between the layers or because nanocomposites do not present ordering anymore. Besides these two well-defined structures, other intermediate organizations can exist showing both intercalation and

Table 2. Pseudo-equilibrium mass uptake (M∞) at the corresponding immersion temperature and heat of dissolution (Hs) for each material

T (°C)	Neat	B1	B3	BM1	BM3
22	0.44	0.54	0.61	0.55	0.62
80	0.71	0.86	0.99	0.88	0.98
93	0.78	0.95	1.09	0.97	1.07
Hs (kJ/mol)	−34.9	−35.0	−34.7	−35.0	−35.2

B1, epoxy–anhydride containing 1 wt% in bentonite; B3, epoxy–anhydride containing 3 wt% in bentonite; BM1, epoxy–anhydride containing 1 wt% in modified bentonite; BM3, epoxy–anhydride containing 3 wt% in modified bentonite.

Table 3. Diffusion coefficient for epoxy clay composites immersed in distilled water (m^2/s)

T (°C)	Neat	B1	B3	BM1	BM3
22	3.00E-13	5.83E-13	6.17E-13	5.67E-13	5.83E-13
80	1.83E-12	3.00E-12	3.67E-12	3.50E-12	3.33E-12
93	5.83E-12	7.50E-12	7.50E-12	3.33E-12	3.33E-12

B1, epoxy–anhydride containing 1 wt% in bentonite; B3, epoxy–anhydride containing 3 wt% in bentonite; BM1, epoxy–anhydride containing 1 wt% in modified bentonite; BM3, epoxy–anhydride containing 3 wt% in modified bentonite.

Table 4. Slope S_H (m/s$^{0.5}$) obtained from linear fitting of stage C in Fig. 6 for each material

T (°C)	Neat	B1	B3	BM1	BM3
22					
80	3.1E-05	2.5E-05	2.5E-05	7.9E-06	7.9E-06
93	4.4E-05	3.9E-05	3.7E-05	1.2E-05	9.8E-06

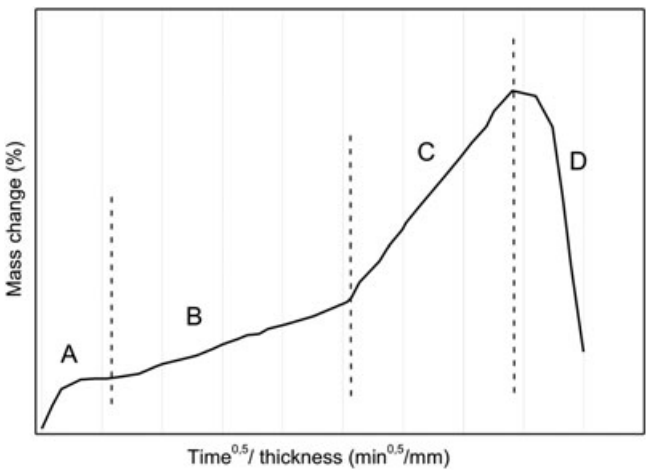

Figure 6. Schematic behavior of epoxy–anhydride water absorption at 93°C.

exfoliation. In this case, a broadening of the diffraction peak is often observed.

X-ray diffraction spectra for bentonite, modified bentonite, and for epoxy–anhydride clay composites are shown in Fig. 1. The bentonite shows a diffraction angle at 6.57° and the modified bentonite at 3.3°. While epoxy-bentonite composites (B1 and B3) are microcomposites due to the presence of a bentonite characteristic pick at 6° in their diffractogram, epoxy-modified bentonite composites could present intercalated-exfoliated morphology because of the absence of the TBHP-bentonite characteristic pick (Fig. 1).[20]

Transmission electron microscopy was used to complete the analysis of the composites morphology. Considering that the dark zones are the silicate platelets, the presence of non-separated bentonite layers (i.e. tactoids) and some areas where the clay layers were not ordered (intercalated zones) are observed (Fig. 2a–c). Similar results were previously reported by other authors.[10,21,22]

From B1 and B3 composites images (Fig. 2a), it is not possible to observe individual layers, and the resulting materials are microcomposites in agreement with XRD results. The higher compatibility between the clay and the matrix, induced by the organic chemical modification, led to a higher degree of delamination or exfoliation.[21] Images for BM1 and BM3 composites present areas where it is possible to recognize individual clay layers corresponding to intercalated-exfoliated morphologies.[23–27]

Water uptake

Figures 3–5 show water uptake at 22°C, 80°C, and 93 °C, respectively. In order to evaluate the service life of installations built with this type of epoxies or composite using them as a matrix, the experimental time frame analyzed goes up to 580 $min^{0.5}$/mm. This experimental window represents the behavior of 23 years of exposure for 6 mm thickness wall of industrial installation, overcoming the 20 years usual industrial service life. The experimental set up was chosen in order to identify the influence of original and modified bentonite on water diffusion mechanism and hydrothermal effects on long-term performance. Moving from short time and low temperature to long time and high temperature, the effect of water diffusion, network relaxation, and the hydrolysis of ester groups can be evaluated. At 22°C, hydrolysis can be neglected, and then, low-temperature water diffusion and network relaxation can be analyzed. On the other side, at high temperature (93°C), hydrolysis rate is high enough to induce network degradation within the period analyzed.[9]

Table 5. Slope S_R ($m/s^{0.5}$) obtained from linear fitting of stage B in Fig. 6 for each material

T (°C)	Neat	B1	B3	BM1	BM3
22	4.3E-07	8.9E-07	8.7E-07	8.9E-07	8.7E-07
80	3.4E-06	3.4E-06	3.5E-06	4.1E-06	4.1E-06
93	NA	8.9E-06	9.4E-06	3.7E-06	3.6E-06

B1, epoxy–anhydride containing 1 wt% in bentonite; B3, epoxy–anhydride containing 3 wt% in bentonite; BM1, epoxy–anhydride containing 1 wt% in modified bentonite; BM3, epoxy–anhydride containing 3 wt% in modified bentonite.

At low temperature (22°C, Fig. 3), the diffusion could be represented by the equilibrium mass content (M∞) and the diffusion coefficient (D). After a linear mass increase observed at short time, a pseudo-equilibrium is reached. This behavior is fulfilled within the first 15 days (150 $mm^{0.5}$/min). However, the pseudo-equilibrium does not hold over an extended period. Neither the neat sample nor the modified ones reach a constant mass over 800 days. Between 15 and 800 days, experimental results show a first-order continuous mass increase. This behavior can be explained in two steps: firstly, a classical diffusion represented by M∞ and D and a second part characterized by linear weight increase. Then, the first part of the process can be analyzed by M∞ and D values reported in Tables 2 and 3. M∞ was determined from the minimum slope of short time (100–150 $mm^{0.5}$/min) gravimetric data, and D was calculated using the solution of Fick's second law (eqn 2) proposed by Shen and Springer.[28]

$$\frac{M_t}{M_\infty} = 1 - \ exp\left[-7,3\left(\frac{D_t}{e^2}\right)^{0,75}\right] \qquad (2)$$

The linear weight increase appearing after a pseudo-equilibrium has been extensively reported for polymers and composite water uptake. Carter and Kibler,[29] for example, explained this behavior dividing water in two different populations: one dissolved in the polymer backbone and hence free of moving and other immobilized in microvoids, both with the possibility of change over time between mobile and immobilized phase. The dual stage diffusion model[30] also explains a linear increase after pseudo-equilibrium by considering mass uptake as the result of Fickian diffusion and network relaxation. The second part of the diffusion curve was analyzed considering the slope (S_R) of the experimental results obtained after the pseudo-equilibrium. The extension of this part is

Table 6. Maximum water content and time to obtain it for epoxy clay composites immersed in distilled water at 80°C and 93°C

	% Maximum absorption		Time at % max. abs			
			80°C		93°C	
	80°C	93°C	$min^{0.5}$/mm	Y6 (1)	$min^{0.5}$/mm	Y6 (1)
B0	4.3	9.1	450	13.8	350	8.4
B1—B3	4.8	6.7	520	18.5	450	13.8
BM1—BM3	3.3	3.2	>580	>23	540	20.0

(1)Y6 time (in years) to obtain maximum water content in a 6 mm thickness wall.

strongly temperature-dependent. While at 22°C, the linear mass increase extends up to the end of the experiment; for the neat sample at 93°C, it practically does not exist. The long-term behavior at higher temperature, 80°C and 93°C, is controlled by the epoxy–anhydride hydrolytic degradation. The epoxy–anhydride curing reaction generates ester groups that are susceptible to suffer hydrolysis. The chemical reaction is a chain scission process that firstly reduces crosslinking density and then produces low molecular weight species. After a short period, water uptake rate increases considerably and eventually the mass decrease by leaching of the low molecular species (alcohols and carboxyl acids). This part of experimental curves are represented by the slope (S_H, Table 4) of the sharper water increase and the time and mass increase at the maximum mass uptake before leaching low molecular weight species.

A schematic curve that represents the water absorption process of epoxy–anhydride systems is presented in Fig. 6. The mass uptake can be divided in four steps. The first one (Fig. 6 zone A) goes from 0 to 100–150 $min^{0.5}$/mm, and it is related with the classical Fickian diffusion.[31] It initiates with a steep linear mass increase and reaches in a short time constant value that can be identified as pseudo-equilibrium. The second part is characterized by a practically constant mass increase. This part could be related with the network viscoelastic relaxation. The third and

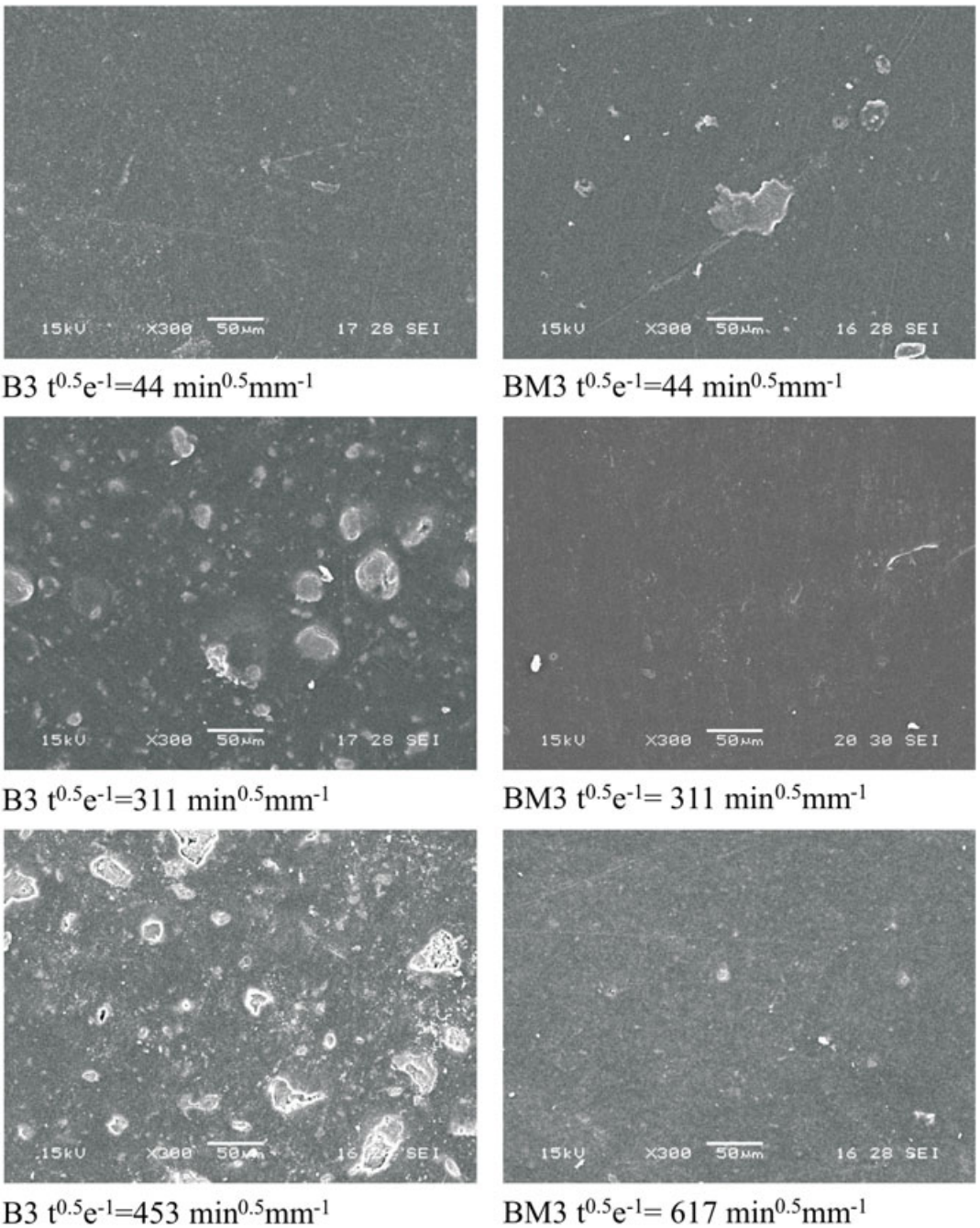

Figure 7. Scanning electron microscopy images of B3 and BM3 surfaces after different exposure times. B3, epoxy clay composite containing 3 wt% in bentonite; BM3, epoxy clay composite containing 3 wt% in TBHP-modified bentonite; TBPH, tributyl hexadecyl phosphonium bromide. [Colour figure can be viewed at wileyonlinelibrary.com]

fourth steps are produced by the same process: epoxy–anhydride chemical degradation by hydrolysis. Hydrolysis could not be observed at low temperature, 22°C, and then steps C and D (Fig. 6) do not exist virtually extending the second part up to equilibrium.

Analyzing the whole set of results, some considerations can be made. For all temperatures, an increase on M∞ was observed for B1, B3, BM1, and BM3. Moreover, M∞ increases with modifier concentration reaching similar values for 1% and 3% of both modifiers. Short-time water absorption depends not only on free volume but also on the number of polar groups where water can be bounded. Several authors have attributed this behavior to the intrinsic hydrophilic clay nature and to the voids resulting of the complex polymer clay composite processing.[14,32] As B and BM are an important source of polar groups, their addition can explain the M∞ increase. The correlation of pseudo-equilibrium absorption with modifier concentration, independently of chemical modification, would indicate a relationship with the number of polar groups present in modified formulations because the modifier (TBHP) does not increase the number of polar groups available for water molecules. In such condition, water bounds not only with network backbone but also with bentonite yielding two kinds of interactions (water-network and water-bentonite).

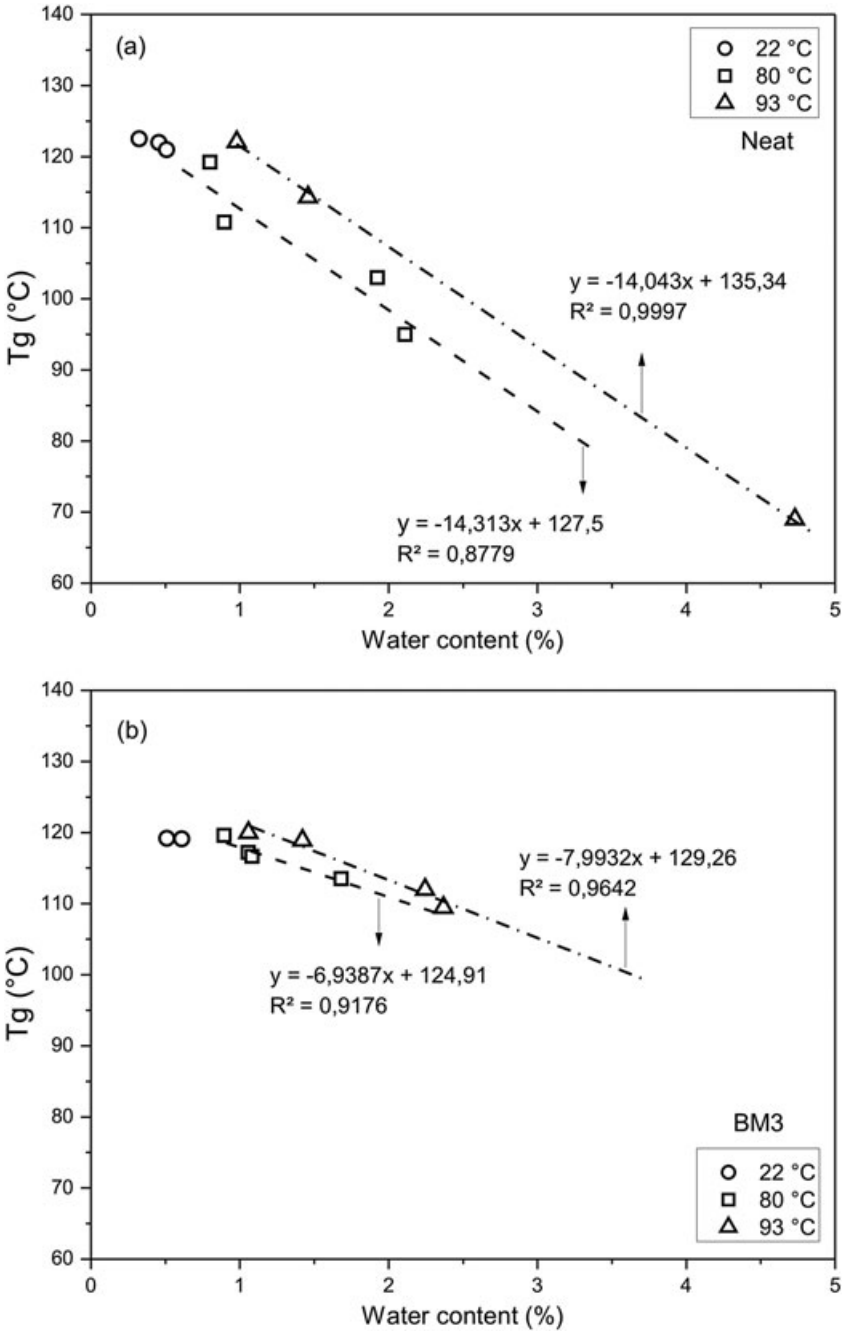

Figure 8. Glass transition temperature (°C) of (a) neat epoxy–anhydride (B0) and (b) BM3 composites as a function of water content (%) at the three immersion temperatures (22°C, 80°C, and 93°C). BM3, epoxy clay composite containing 3 wt% in TBHP-modified bentonite; TBPH, tributyl hexadecyl phosphonium bromide.

In order to evaluate the water-network interaction, the heat of dissolution (Hs) can be analyzed. From the correlation of M∞ versus the temperature proposed by Merdas *et. al.*,[33] the Hs for each sample was calculated (Table 2). The results show that the modifier addition does not produce differences in the average solid–water interaction. In summary, bentonite and modified bentonite increase the active sites for water interaction, but water-polymer and water-bentonite interaction would produce similar strength bonds according to the heat of dissolution evaluated.

Tables 3 and 5 show the influence of bentonite and its modification from low-temperature predominating process (diffusion) to high-temperature prevailing one (hydrolysis). For low temperature and short time, diffusivity is higher in modified samples (B1, B3, BM1, and BM3) than in the neat epoxy. Although the relationship between hydrophilicity and diffusion can be generally described by "the higher the hydrophilicity, the slower the diffusion"[33], there are also results showing the opposite effect.[34] A joint increase in M_∞ and D can be a consequence of transportation rate kinetically controlled by local scale segmental motion, and thus modified samples would present a higher topology change because of a better short-range chain flexibility. Because the bentonite and modified bentonite addition do not change interaction strength, faster local molecular rearrangements would explain the D increases in modified samples.

From 80°C to 93°C, BM samples diffusion coefficient show no change with temperature; the same behavior can be observed in S_R. Short-time diffusion and relaxation seems to be closely related, both associated to local motion rate. Increasing temperature from 80°C to 93°C, both D and S_R increase by a factor between two and three in neat, B1, and B3 samples. Meanwhile, between 80°C and 93°C, D and S_R remain constant in BM samples. Clearly, this observation is the result of two simultaneous and opposite effects. At 22°C and 80°C, the faster local molecular rearrangements prevails. At 93°C, the clay layers dispersed in the nanometer scale in the matrix can decrease the mean free path of water molecules to pass through the nanocomposite network compared with the pure matrix, which leads to lower diffusivity.[15]

Finally, the mass uptake slope of the step related with hydrolysis (S_H) is clearly lower in BM samples, while neat and B samples show similar values. Hydrolysis reaction requires that a water molecule find a hydrolyzable point (ester group). Because water interaction (Hs) does not depend on modifier or on its concentration, part of the water interacts with bentonite instead of polymer network, diminishing the amount of water that is able to participate in hydrolysis. The decrease in water-reactive site concentration decreases hydrolysis rate extending service life (Table 6). This effect is influenced by modified distribution; therefore, BM shows a higher decrease in hydrolysis rate because of its nanoscale distribution.

Surface morphology

Long-term gravimetric results show that modified bentonite slows down the chemical degradation of epoxy–anhydride even if they do not inhibit it. The water inlet in the matrix is enough to let the hydrolysis occur, eventually leading to catastrophic mass loss. SEM images show a great change in the surface morphology of bentonite-modified filled composites (BM3) in comparison with bentonite composites (B3) at intermediate and long times for samples immersed at 93°C (Fig. 7). Morphology change is related with the surface degradation observed as an important increase in deteriorated areas. The time frame is consistent between this deteriorated areas appearance and the mass uptake inflection considered before the beginning of the third step (C). The surface degradation observed can be responsible of an autocatalytic process by the increasing of the sample surface in contact with water.

Glass transition temperature

The glass transition temperature is an important parameter that influences water diffusion in polymers. It is well known[35] that water could act as a plasticizer in thermosetting polymers decreasing the glass transition temperature. In epoxy–anhydride systems, water can also induce hydrolytic degradation. Each hydrolysis event implies a chain scission and, as consequence, polymer cross-linked density decrease as well.[36] As the Tg increases as a function of the cross-linking density, the decrease on this temperature could be related with either plasticization and/or water degradation by hydrolysis. As an example, Fig. 8a and b shows the variation of neat and BM3 Tg values as a function of the mass increase (Tg values before immersion are shown in Table 7). It can be observed that at 80°C and 93°C, BM3 samples not only show a lower mass uptake but also a lower slope in the curve of Tg versus mass uptake. The influence of the reduction on the glass transition temperature on both the absorption and hydrolysis processes can be critical when Tg is getting closer to the diffusion temperature and much stronger if the temperature of the experiment is higher than Tg. In the case of the neat samples, Tg falls up to close to 70°C, which means that during the diffusion process, polymer changes from glassy to rubbery state. Then, the high degradation rate observed in neat samples together with the time reduction to initiate hydrolysis is due to a combined effect between the high water-network concentration and the higher decrease in Tg produced by water plasticization (Fig. 8a and b). Figure 8 shows that when neat samples reach a 2.5% mass increase, Tg decreases up to 90°C. This means that an important part of the experiment occurs in rubbery state, which increases backbone mobility considerably. The increase in network mobility and free volume produces the autocatalytic

Table 7. Glass transition temperature (Tg) and flexural modulus (E) for the studied materials before immersion

	B0	B1	B3	BM1	BM3
Tg (°C)	129	131	131	130	130
E (GPa)	3.48 ± 0.07	3.88 ± 0.15	3.98 ± 0.04	3.65 ± 0.12	3.68 ± 0.13

B0, neat epoxy-anhydrite; B1, epoxy–anhydride containing 1 wt% in bentonite; B3, epoxy–anhydride containing 3 wt% in bentonite; BM1, epoxy–anhydride containing 1 wt% in modified bentonite; BM3, epoxy–anhydride containing 3 wt% in modified bentonite.

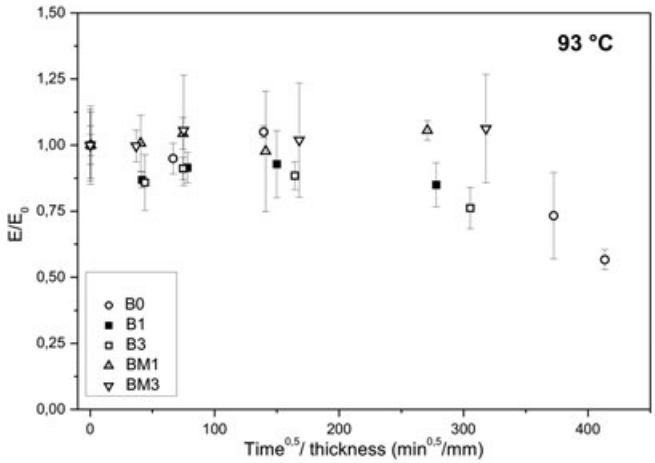

Figure 9. Flexural modulus ratio (E/E0) between the dry samples (E0) and samples that were immersed in water at 93°C (E) as a function of the reduced time ($min^{0.5}$/mm).

degradation process. On the other side, in modified samples, the slope of Tg versus mass uptake is milder. The effect of mass uptake in Tg reduction can be explained by a decrease in matrix water content because part of the water would be bound to clay particles.

Flexural modulus

Finally, flexural modulus (E) was measured for the five systems (Table 7) at the three conditions studied (Fig. 9). Although it was observed that E is slightly higher for epoxy clay composites than for neat epoxy, the difference is not significant. In view of the results, the water degradation at the three temperatures studied do not affect considerably the materials E during the first 25 days of immersion. However, after 100 days at 93°C, the E of bentonite composites falls in comparison with the modified-bentonite composite. This fact is consistent with the results observed in gravimetric data and with the analysis of glass transition temperature.

CONCLUSIONS

Epoxy–anhydride/clay composites were prepared using bentonite in 1 and 3 wt% (hereinafter B1 and B3) and TBHP modified-bentonite in 1 and 3 wt% (hereinafter BM1 and BM3) in order to improve hydrolytic degradation resistance. Using unmodified bentonite (B1 and B3), a microcomposite morphology was obtained, meanwhile TBHP modifier increases bentonite-epoxy compatibility producing a nanoscale bentonite distribution. Composites were characterized by X-ray diffraction (XRD) and TEM, and their water absorption behavior were studied at three different temperatures (22°C, 80°C, and 93 °C). The filler effect in water absorption and thermal and mechanical behavior was analyzed.

Short-term water uptake shows that the addition of bentonite and TBHP-bentonite increases M∞ and D. This result would be due to transportation rate kinetically controlled by local scale segmental motion. Modification increases short-range chain flexibility and consequently generates higher topology change. Because bentonite and TBHP-bentonite addition do not change the interaction strength with water molecules, faster local molecular rearrangements would explain the D increases in modified samples.

TBHP-bentonite samples present a clear improvement in long-term water uptake performance. The mass uptake at longer time is the related hydrolytic epoxy–anhydride degradation. The nanoscale morphology obtained in TBHP-bentonite composites decreases the concentration of water molecules in contact with network backbone, which is confirmed by a smoother Tg versus mass uptake decrease. The decrease in water-reactive site concentration decreases hydrolysis rate extending service life. On the other hand, the high degradation rate observed in neat samples together with the shorten time to initiate hydrolysis is because of a cascade effect initiated by the increase in water-network concentration, which produces a steep decrease in Tg due to water plasticization. When Tg is similar, or even lower than 93°C, backbone mobility increases considerably.

Finally, TBHP-modified bentonite composites present a great enhancement when materials suffer chemical degradation by water at high temperatures. BM3 delayed the effects of hydrolysis extending the time scale to 160%. The use of TBHP-bentonite as epoxy–anhydride modifier would be an interesting material to be used as matrix for high-temperature composite pipeline.

Acknowledgements

The authors acknowledge the support from FONARSEC (Agencia Nacional de Promoción Científica y Tecnológica), CONICET, and Universidad Nacional de Mar del Plata.

REFERENCES

[1] Q. Jia, M. Zheng, H. X. Chen, R. J. Shen, *Polym. Bull.* **2005**, *54*, 65.
[2] [2] M. R. Bagherzadeh, T. Mousavinejad, *Prog. Org. Coat.* **2012**, *74*, 589.
[3] K. Kowalczyk, T. Spychaj, *Prog. Org. Coat.* **2008**, *62*, 425.
[4] Z. Ahmad, M. P. Ansell, D. Smedley, *Int. J of Adhes. Adhes.* **2010**, *30*, 448.
[5] B. De, N. Karak, *J of Appl. Pol. Sci.* **2014**, *131*, 40327.
[6] T. Braun, F. Hausel, J. Bauer, O. Wittler, R. Mrossko, M. Bouazza, K. F. Becker, U. Oestermann, M. Koch, B. Bader, C. Minge, R. Aschenbrenner, H. Reichl, Nano-particle enhanced encapsulants for improved humidity resistance. *Electronic Components and Technology Conference*, Lake Buena Vista, Fl, USA, **2008**.
[7] M. K. Antoon, J. L. Koenig, *J. Polym. Sci. Part B Polym. Phys.* **1981**, *19*, 197.
[8] J. El Yagoubi, G. Lubineau, A. Traidia, J. Verdu, *Compos. Part A Appl. Sci. Manuf.* **2015**, *68*, 184.
[9] M. Al-Qadhi, N. Merah, Z. M. Gasem, *J. Mater. Sci.* **2013**, *48*, 3798.
[10] O. Becker, R. J. Varley, G. P. Simon, *Euro. Polym. J.* **2004**, *40*, 187.
[11] M. Al-Qadhi, N. Merah, Z. M. Gasem, N. Abu-Dheir, B. J. Aleem, *Polym. Compos.* **2014**, *35*, 318.
[12] T. Glaskova, A. Aniskevich, *Comp. Sci. Tech.* **2009**, *69*, 2711.
[13] L. Wang, K. Wang, L. Chen, C. He, Y. Zhang, *Polym. Eng. Sci.* **2006**, *46*, 215.
[14] B. Abu-Jdayil, K. Al-Malah, R. Sawalha, *J. Reinf. Plast. Comp.* **2002**, *21*, 1597.
[15] R. Ollier, E. Rodriguez, V. Alvarez, *Comp. Part A* **2013**, *48*, 137.
[16] J. C. Roelofs, P. H. Berben, *App. Clay Sci.* **2006**, *33*, 13.
[17] P. Capkova, M. Pospisi, M. Valaskova, D. Merinska, M. Trchova, Z. Sedlakova, Z. Weiss, J. Simonik, *J. Colloid and Interf. Sci.* **2006**, *300*, 264.
[18] R. Ollier, A. Vazquez, V. Alvarez, in *Advances in Nanotechnology*, 10, (Eds: Z. Bartul, J. Tremor). Nov. Publ., New York, **2011**, 281-301.
[19] M. E. Penoff, M. Lanfranconi, V. A. Alvarez, R. Ollier, *Thermochim. Acta* **2015**, *608*, 20.
[20] M. Alexarder, P. Dubois, *Mater. Sci. Eng.* **2000**, *28*, 1.
[21] H. R. Dennis, D. L. Hunter, D. Chang, S. Kim, J.,. L. White, J. W. Cho, *Polymer* **2001**, *42*, 9513.

[22] M. Modesti, A. Lorenzetti, D. Bon, S. Besco, *Polymer* **2005**, *46*, 10237.
[23] Z. Martin, I. Jimenez, M. A. Gomez, H. W. Ade, D. A. Kilcoyne, D. Hernadez Cruz, *J. Phys. Chem. B* **2009**, *113*, 11160.
[24] N. N. Bhiwankar, R. A. Weiss, *Polymer* **2006**, *47*, 6684.
[25] S. Varghese, J. Karger-Kocsis, *Polymer* **2003**, *44*, 4921.
[26] D. Garcia Lopez, I. Gobernado Mitre, J. F. FernandeZ, J. C. Merino, J. M. Pastor, *Polymer* **2005**, *46*, 2758.
[27] S. Varghese, J. Karger-Kocsics, *Polymer* **2003**, *44*, 3977.
[28] C. H. Shen, G. S. Springer, *J Compos Mater* **1976**, *10*, 2.
[29] H. G. Carter, K. G. Kibler, *J. Comp. Mater.* **1978**, *12*, 118.
[30] M. D. Placette, X. Fan, J. H. Zhao, D. Edwards, In thermal, mechanical and multi-physics simulation and experiments in microelectronics and microsystems (EuroSimE), 12th International Conference on. IEEE, **2011**.
[31] J. Crank, The mathematics of diffusion, London. (**1975**).
[32] N. Rull, R. Ollier, G. Francucci, E. Rodriguez, V. Alvarez, *J. Comp. Mater.* **2015**, *49*, 1629.
[33] I. Merdas, A. Tcharkhtchi, F. Tominette, J. Verdu, K. Dean, W. Cook, *Polymer* **2002**, *43*, 4619.
[34] L. Li, S. Zhang, Y. Chen, M. Liu, Y. Ding, X. Luo, *Chem. Mater.* **2005**, *17*, 839.
[35] L. W. Jelinsky, J. J. Dumais, A. L. Cholli, T. S. Ellis, F. E. Karasf, *Macromolecules* **1985**, *18*, 1091.
[36] E. Richaud, P. Gilormini, M. Coquillat, J. Verdu, *Macrom. Theory and Simul.* **2014**, *23*, 320.

